ROYAL SOCIETY OF CHEMISTRY

PAPER

Check for updates

Shearinines U–Y, indole diterpenoids from an entomogenous fungus, *Penicillium* sp.†

Peinan Fu, [ID][a] Feng Guo,[a] Tingnan Zhou,[b] Hongxia Bei,[a] Huiling Tang,[a] Jiaxin Li[a] and Zhiyang Lv*[a]

Five new indole diterpenoids, shearinines U–Y (**2**–**6**), and the known compound 22,23-dehydro-shearinine A (**1**) were isolated from cultures of the entomogenous fungus *Penicillium* sp. Their structures were elucidated primarily by NMR experiments. The absolute configurations of **2**–**6** were assigned by electronic circular dichroism calculations, respectively. Compounds **1**–**3** showed moderate cytotoxicity, with IC_{50} values of 11.7–26.2 μM.

Introduction

Indole diterpenoids (IDTs) represent a class of structurally diverse and biologically active natural products.[1,2] Most reported IDTs are isolated from fungi within the genera *Penicillium*,[3–5] *Aspergillus*,[6] *Claviceps*,[7] and *Epichloe*.[8] These intriguing molecules are characterized by a fused diterpenoid backbone and an indole ring, which can be further elaborated through cyclization, oxidation, and prenylation to yield a plethora of complex architectures.[9–12] These natural products have been reported to exhibit a range of biological activities, such as antibacterial, antifungal, antitumor, and antiviral effects.[13–17]

The species of fungal genus *Penicillium* are known to be prolific producers of highly diverse secondary metabolites, which contribute to their multifaceted biological profiles.[18–22] During our continuous search for new cytotoxic metabolites from the entomogenous fungus fungi,[23–25] a strain of *Penicillium* sp., isolated from a wheat cyst nematode in Xiao County, Anhui, People's Republic of China, was grown in a solid-substrate fermentation culture. An ethyl acetate (EtOAc) extract of the culture showed cytotoxic effects towards a small panel of four tumor cell lines. Fractionation of the extract afforded five new indole diterpenoids, which we named shearinines U–Y (**2**–**6**; Fig. 1), and the known compound 22,23-dehydro-shearinine A (**1**; Fig. 1). Details of the isolation, structure elucidation, and cytotoxicity evaluation of these compounds are reported herein.

[a] *School of Pharmacy, Jiangsu Food and Pharmaceutical Science College, Huaian 223003, People's Republic of China. E-mail: lvpharm@163.com*

[b] *Institute of Medicinal Biotechnology, Chinese Academy of Medical Sciences & Peking Union Medical College, Beijing 100730, People's Republic of China*

Results and discussion

The known compound **1** was identified as 22,23-dehydro-shearinine A by comparison of its MS and NMR data (Fig. S55 and S56†) with those previously reported.[26]

Shearinine U (**2**) was assigned a molecular formula of $C_{37}H_{43}NO_5$ by HRESIMS, indicating 17° of unsaturation. The ^{1}H and ^{13}C NMR data for **2** (Tables 1 and 2) closely resembled those for **1**, apart from two additional hydroxy signals resonating at δ_H 6.55 and 4.31. The HMBC correlations from OH-7 to C-7 and C-12, from OH-34 to C-9 and C-34 suggested cleavage of the 1,3-dioxolane ring in the structure of **1**. Moreover, **2** displays an olefinic signal (a sp^2 carbon at δ_C 140.7 and δ_H 6.06/δ_C 130.4), instead of a 13-OH group, that were assigned to the double bond at $\Delta^{13(14)}$, which was confirmed by the HMBC correlation from H_2-15 to C-13. On the basis of these data, the planar structure of **2** was elucidated.

The relative configuration of **2** was proposed by analysis of NOESY correlations (Fig. 2 and 3). NOESY correlations of H-16 with H-17a and H_3-33 indicated that these protons are all on the same face of the ring system, whereas those of H-17b with
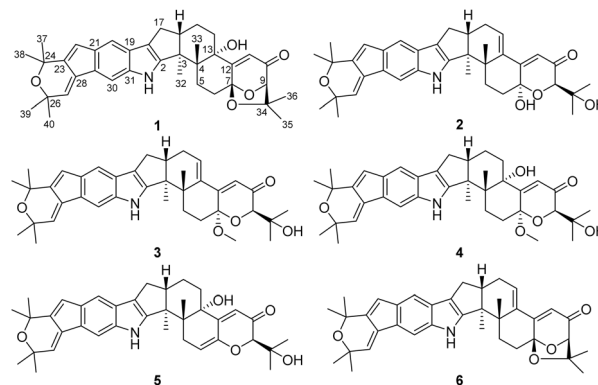

Fig. 1 Structures of compounds **1**–**6**.

Table 1 ^{1}H NMR data of **2–6**

No.	**2** $\delta_H{}^a$ (J in Hz)	**3** $\delta_H{}^a$ (J in Hz)	**4** $\delta_H{}^a$ (J in Hz)	**5** $\delta_H{}^a$ (J in Hz)	**6** $\delta_H{}^a$ (J in Hz)
5a	2.06, m	1.92, m	2.39, m	3.00, brd (16.5)	1.98, m
5b		1.81, m		2.41, dd (17.3, 6.2)	
6a	2.08, m	2.08, m	2.49, m	5.64, m	1.84, m
6b		1.97, m	1.87, m		
9	4.14, s	3.92, s	3.92, s	4.02, s	4.43, s
11	5.85, s	5.90, s	5.78, s	5.80, s	6.15, s
14	6.06, dd (5.0, 2.3)	6.03, dd (5.0, 2.3)	1.78, m	1.93, m	6.52, dd (4.9, 2.6)
			1.66, m	1.82, m	
15	2.27, m	2.27, m	1.91, m	1.92, m	2.38, m
			1.60, m	1.65, m	
16	2.80, m	2.81, m	2.71, m	2.70, m	2.87, m
17	2.74, dd (13.0, 6.7)	2.74, dd (13.0, 6.7)	2.60, dd (12.9, 6.1)	2.60, dd (12.9, 6.2)	2.73, dd (13.2, 6.7)
	2.37, dd (13.0, 10.1)	2.38, dd (13.0, 10.2)	2.30, dd (12.9, 11.4)	2.31, dd (12.9, 11.4)	2.37, dd (13.2, 10.6)
20	7.11, s	7.11, s	7.07, s	7.07, s	7.11, s
22	6.44, d (1.8)	6.45, d (1.8)	6.43, d (1.7)	6.43, d (1.2)	6.45, d (1.6)
27	6.74, d (1.8)	6.74, d (1.8)	6.71, d (1.7)	6.71, d (1.2)	6.74, d (1.6)
30	7.49, s	7.50, s	7.46, s	7.47, s	7.52, s
32	0.92, s	0.90, s	1.25, s	1.29, s	0.97, s
33	1.09, s	1.12, s	0.94, s	1.01, s	1.17, s
35	1.19, s	1.23, s	1.23, s	1.13, s	1.39, s
36	1.19, s	1.22, s	1.20, s	1.25, s	1.14, s
37	1.45, s	1.46, s	1.45, s	1.45, s	1.46, s
38	1.45, s	1.46, s	1.45, s	1.45, s	1.46, s
39	1.40, s	1.40, s	1.39, s	1.39, s	1.39, s
40	1.40, s	1.40, s	1.39, s	1.39, s	1.40, s
1-NH	10.86, s	10.87, s	10.74, s	10.76, s	10.87, s
7-OH	6.55, s				
7-OMe		3.26, s	3.37, s		
13-OH			4.57, s	4.90, s	
34-OH	4.31, s	4.40, s	4.45, s	4.54, s	

^{a} Recorded at 600 MHz.

H$_3$-32 placed the protons on the opposite face. The other NOESY correlations of OH-7 with H-9 placed these protons on the same face. Therefore, the relative configuration of **2** was deduced as shown.

The absolute configuration of **2** was deduced by comparison of the experimental and simulated electronic circular dichroism (ECD) spectra calculated using the time-dependent density functional theory (TDDFT).[27] The ECD spectra of the four possible isomers **2a–d** (Fig. S11†) were calculated. A systematic conformational analysis was performed for **2a–d** with the Molecular Operating Environment (MOE) software package using the MMFF94 molecular mechanics force field calculation. The selected conformers were then reoptimized using TDDFT at the B3LYP/6-311G(d,p) level to afford the lowest energy conformers. The conformers were further filtered based on the Boltzmann-population rule, resulting in one significant conformer for each configuration (Fig. S11†). The overall calculated ECD spectra of **2a–d** were then generated by Gaussian broadening (Fig. 4). The experimental ECD curve of **2** was nearly identical to that calculated for **2a**, suggesting the 3S,4S,7S,9R,16S absolute configuration for **2**.

The molecular formula of Shearinine V (**3**) was determined to be C$_{38}$H$_{45}$NO$_5$ (17° of unsaturation) based on HRESIMS and the

NMR data (Tables 1 and 2), which is 14 mass units higher than that of **2**. Analysis of the ^{1}H and ^{13}C NMR data for **3** revealed the presence of structural features similar to those found in **2**, except that OH-7 (δ_H 6.55) was replaced by a methoxy unit (δ_H/δ_C 3.26/48.5), and this observation was supported by the HMBC correlations from these newly observed methoxy protons to C-7. Therefore, the gross structure of **3** was established. The relative configuration of **3** was also deduced by analysis of NOESY data, and by analogy to **2**. The ECD spectrum of **3** was nearly identical to that of **2** (Fig. S10 and S21†), indicating that the absolute configuration of **2** was the same as that of **2**.

Shearinine W (**4**) was assigned a molecular formula of C$_{38}$H$_{47}$NO$_6$ (16° of unsaturation) by HRESIMS and the NMR data (Tables 1 and 2), which is 18 mass units higher than that of **3**, except that the C-13 oxygenated tertiary carbons (δ_C 75.6) units and C-14 methylene (δ_H/δ_C 1.78, 1.66/32.5) in **4** instead of an olefin moiety in **3**, which was confirmed by the HMBC correlations from H-11 to C-13 and from 13-OH to C-12 and C-13. Therefore, the gross structure of **4** was proposed.

The relative configuration of **4** was also proposed by analysis of NOESY correlations (Fig. 3). The NOESY correlations of H$_3$-32 with 13-OH revealed that these protons are all on the same face of the ring system. The relative configuration of other

Table 2 NMR data of **2–6**

No.	2 $\delta_C{}^a$, type	3 $\delta_C{}^a$, type	4 $\delta_C{}^a$, type	5 $\delta_C{}^a$, type	6 $\delta_C{}^a$, type
2	148.9, qC	148.8, qC	152.8, qC	152.9, qC	148.7, qC
3	47.9, qC	47.9, qC	50.4, qC	50.3, qC	49.0, qC
4	42.1, qC	42.0, qC	42.3, qC	42.8, qC	38.9, qC
5	28.1, CH₂	26.7, CH₂	24.8, CH₂	30.6, CH₂	29.0, CH₂
6	32.9, CH₂	27.4, CH₂	27.2, CH₂	110.9, qC	30.6, CH₂
7	93.5, qC	96.5, qC	97.0, qC	145.1, qC	103.9, qC
9	78.3, CH	78.6, CH	78.4, CH	85.9, CH	87.4, CH
10	198.7, qC	197.1, qC	197.0, qC	195.1, qC	195.1, qC
11	120.7, CH	121.2, CH	121.2, CH	116.0, CH	117.6, CH
12	161.4, qC	159.8, qC	160.2, qC	154.5, qC	163.9, qC
13	140.7, qC	140.5, qC	75.6, qC	73.9, qC	138.4, qC
14	130.4, CH	130.7, CH	32.5, CH₂	31.8, CH₂	132.9, CH
15	27.5, CH₂	27.5, CH₂	20.9, CH₂	21.1, CH₂	28.2, CH₂
16	44.9, CH	44.9, CH	49.1, CH	49.2, CH	44.7, CH
17	26.7, CH₂	26.3, CH₂	26.8, CH₂	27.0, CH₂	26.8, CH₂
18	117.0, qC	117.0, qC	115.8, qC	115.9, qC	117.1, qC
19	124.2, qC	124.1, qC	124.3, qC	124.5, qC	124.2, qC
20	109.8, CH	109.7, CH	109.5, CH	109.6, CH	109.7, CH
21	135.5, qC	135.5, qC	135.3, qC	135.3, qC	135.6, qC
22	121.3, CH	121.3, CH	121.2, CH	121.3, CH	121.3, CH
23	140.9, qC	140.9, qC	140.7, qC	140.9, qC	141.0, qC
24	72.5, qC	72.5, qC	72.3, qC	72.5, qC	72.5, qC
26	72.4, qC	72.4, qC	72.2, qC	72.4, qC	72.4, qC
27	129.1, CH	129.1, CH	128.6, CH	128.9, CH	129.1, CH
28	133.5, qC	133.5, qC	133.4, qC	133.5, qC	133.5, qC
29	127.6, qC	127.6, qC	127.0, qC	127.2, qC	127.6, qC
30	104.9, CH	104.9, CH	104.7, CH	104.9, CH	105.8, CH
31	138.5, qC	138.5, qC	137.7, qC	138.0, qC	138.5, qC
32	15.0, CH₃	15.0, CH₃	16.2, CH₃	16.5, CH₃	14.4, CH₃
33	22.5, CH₃	22.6, CH₃	19.0, CH₃	19.7, CH₃	27.5, CH₃
34	71.4, qC	71.1, qC	70.9, qC	73.0, qC	77.7, qC
35	26.5, CH₃	26.0, CH₃	26.1, CH₃	26.8, CH₃	28.8, CH₃
36	25.8, CH₃	26.0, CH₃	25.6, CH₃	27.1, CH₃	22.9, CH₃
37	31.4, CH₃	31.4, CH₃	31.3, CH₃	31.4, CH₃	31.5, CH₃
38	31.4, CH₃	31.4, CH₃	31.3, CH₃	31.5, CH₃	31.4, CH₃
39	30.7, CH₃	30.7, CH₃	30.6, CH₃	30.8, CH₃	30.8, CH₃
40	30.7, CH₃	30.7, CH₃	30.6, CH₃	30.7, CH₃	30.7, CH₃
7-OMe		48.5, CH₃	48.8, CH₃		

^{a} Recorded at 150 MHz.
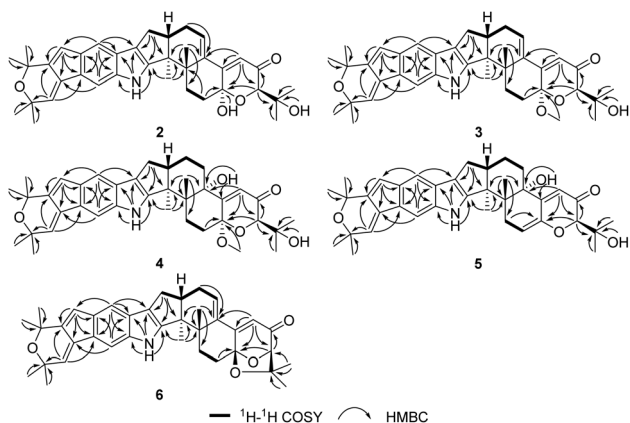
Fig. 2 Key ^{1}H–^{1}H COSY and HMBC correlations of **2–6**.
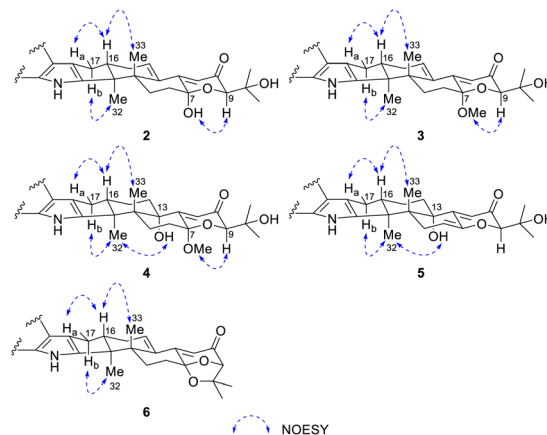
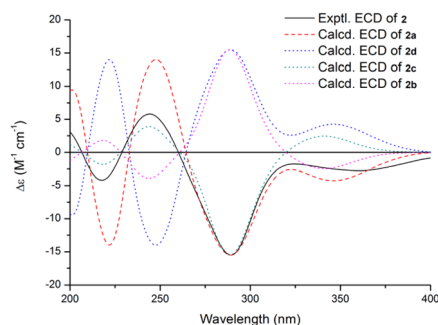**Fig. 3** Key NOESY correlations of **2–6**.

Fig. 4 Experimental ECD spectrum of **2** in MeOH and the calculated ECD spectra of **2a–d**.

stereogenic centers were proposed in a similar fashion to **2** and **3** as shown in Fig. 3. The absolute configuration for **4** was also deduced by comparison of the experimental and calculated ECD spectra for the four possible enantiomers **4a–d**. The lowest energy conformers for **4a–d** were generated by Gaussian broadening (Fig. 5). The experimental ECD spectrum of **4** matched reasonably well with the calculated one for **4a**, suggesting that **4** has the 3S,4R,7S,9R,13S,16S absolute configuration.

Shearinine X (**5**) was determined to have a molecular formula of $C_{37}H_{43}NO_5$ (17° of unsaturation) based on HRESIMS and the
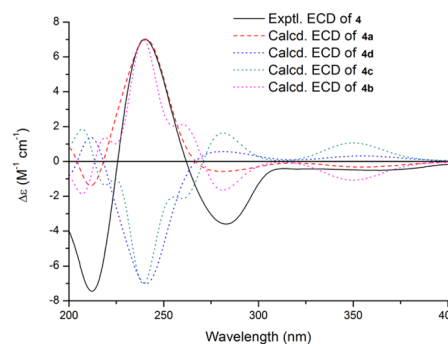

Fig. 5 Experimental ECD spectrum of **4** in MeOH and the calculated ECD spectra of **4a–d**.
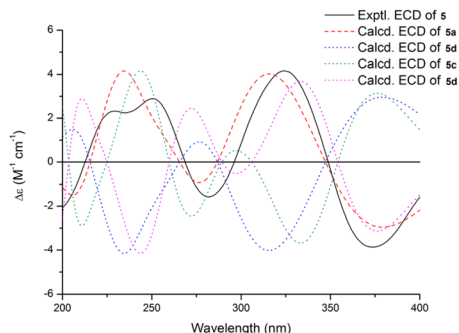
Fig. 6 Experimental ECD spectrum of **5** in MeOH and the calculated ECD spectra of **5a–d**.

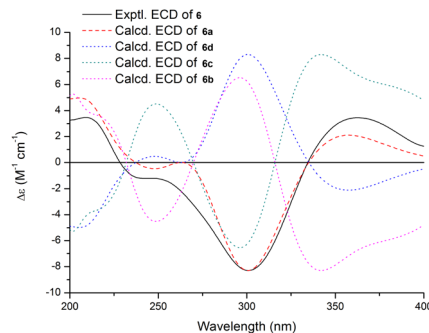**Fig. 7** Experimental ECD spectrum of **6** in MeOH and the calculated ECD spectra of **6a–d**.

NMR data (Tables 1 and 2). The ^{1}H and ^{13}C NMR spectra of **5** showed resonances similar to those of **4**, revealed that **5** displays an olefinic signal (δ_H 5.64/δ_C 110.9 and a sp^2 carbon at δ_C 145.1), instead of a 7-OMe group, that were assigned to the double bond at $\Delta^{6(7)}$, accounting for the additional degree of unsaturation of **5**, which was confirmed by the HMBC correlation from H-5 to C-7. The relative configurations of all stereogenic centers in **5** were proposed to be the same as their counterparts in **4** by analysis of the NOESY data (Fig. 3) for relevant protons, and the absolute configuration was deduced to be 3S,4R,9R,13S,16S based on the results of experimental and calculated ECD (Fig. 6).

On the IR spectra, the higher wavenumber region of the spectrum of compounds **2–5** did not contain a diagnostic strong and sharp band above 3200 cm^{-1} that is typical of the N–H stretching vibration of an indole N–H group. Instead, a very broad band was attributed to the O–H (H-bonded).[28]

Shearinine Y (**6**) gave a molecular formula of $C_{37}H_{41}NO_4$ (18° of unsaturation) by analysis of its HRESIMS and the NMR data (Tables 1 and 2), which is 18 mass units less than that of **2**. Analysis of the ^{1}H and ^{13}C NMR data for **6** revealed the presence of structural features similar to those found in **2**, except that 7-OH (δ_H 6.55) and 34-OH (δ_H 4.31) were absent. Considering the unsaturation requirement for **6**, allowed the deduction of a dioxolane moiety fused to the pyranone at C-7 and C-9. Therefore, the gross structure of **6** was established. The relative configuration of **6** was deduced as shown by analysis of the NOESY correlations (Fig. 3) and by analogy to **2**, and the absolute configuration of **6** was further determined by comparison of the experimental and calculated ECD spectra. The experimental ECD of **6** correlated well to the calculated curve of **6a** (Fig. 7), suggesting the 3S,4S,7S,9R,16S absolute configuration.

An additional experiment was performed to exclude the possibility that **3** and **4** are artifacts arising from their corresponding analogues during the isolation process. For this purpose, EtOAc extract were soaked in acetonitrile, and then analyzed by HPLC with CH$_3$CN–H$_2$O, which was found that there were still **3** and **4** peaks in the fermentation products. The result indicated that the new methoxylated analogues **3** and **4** are true natural products and not artifacts formed through methylation when using MeOH (Table 3).

Compounds **1–6** were tested for cytotoxicity against four tumor cell lines, Huh7 (human hepatocellular carcinoma cells),

Table 3 Cytotoxicity of compounds **1–3**

Compound	IC$_{50}$^{a} (μM)			
	Huh7	SKBR3	A549	MB49
1	11.7 ± 2.0	26.2 ± 3.5	22.0 ± 2.1	18.6 ± 2.3
2	11.8 ± 2.2	21.8 ± 4.0	22.1 ± 2.7	17.1 ± 0.8
3	18.1 ± 4.0	21.0 ± 4.8	NA^b	NA^b
Cisplatin^c	5.2 ± 0.7	3.7 ± 0.5	6.5 ± 0.5	1.6 ± 0.4

^{a} IC$_{50}$ values were averaged from at least three independent experiments. ^{b} No activity was detected at 50 μM. ^{c} Positive control.

SKBR3 (human breast cancer cells), A549 (human lung adeno-carcinoma cells), and MB49 (mouse bladder carcinoma cells).[29] Compounds **1–3** showed moderate cytotoxic effects, with IC$_{50}$ values of 11.7–26.2 μM (the positive control cisplatin showed IC$_{50}$ values of 1.6–6.5 μM). However, compounds **4–6** did not show detectable activity at 50 μM.

Experimental

General experimental procedures

Optical rotations were measured on a Rudolph Research Analytical automatic polarimeter, and UV data were recorded on a Shimadzu Biospec-1601 spectrophotometer. CD spectra were recorded on a JASCO J-815 spectropolarimeter. IR data were recorded using a Nicolet Magna-IR 750 spectrophotometer. ^{1}H and ^{13}C NMR spectra were acquired with Bruker Avance III-600 spectrometers using solvent signals (DMSO-d_6: δ_H 2.50/δ_C 39.52) as references. The HSQC and HMBC experiments were optimized for 145.0 and 8.0 Hz, respectively. ESIMS and HRESIMS data were obtained on an Agilent Accurate-Mass-Q-TOF LC/MS G6550 instrument equipped with an ESI source. HPLC analysis and separation were performed using an Agilent 1260 instrument equipped with a variable-wavelength UV detector.

Fungal material

The culture of *Penicillium* sp. was isolated from a wheat cyst nematode collected in Xiao County, Anhui, People's Republic of China, in 2009. The isolate was identified based on morphology and sequence (GenBank accession no. ON307320)

analysis of the ITS region of the rDNA. The fungal strain was cultured on slants of potato dextrose agar (PDA) at 25 °C for 10 days. Agar plugs were cut into small pieces (about $0.5 \times 0.5 \times 0.5$ cm^3) under aseptic conditions, and 25 pieces were used to inoculate in five 250 mL Erlenmeyer flasks, each containing 50 mL of media (0.4% glucose, 1% malt extract, and 0.4% yeast extract), and the final pH of the media was adjusted to 6.5 and sterilized by autoclave. Five flasks of the inoculated media were incubated at 25 °C on a rotary shaker at 170 rpm for 5 days to prepare the seed culture. Fermentation was carried out in 40 Fernbach flasks (500 mL) each containing 80 g of rice. Distilled H_2O (120 mL) was added to each flask, and the contents were soaked overnight before autoclaving at 15 psi for 30 min. After cooling to room temperature, each flask was inoculated with 5.0 mL of the spore inoculum and incubated at 25 °C for 25 days.

Extraction and isolation

The fermentation material was extracted repeatedly with EtOAc (4×6.0 L), and the organic solvent was evaporated to dryness under vacuum to afford 20.6 g of crude extract. The crude extract was fractionated by silica gel vacuum liquid chromatography (VLC) using petroleum ether–CH_2Cl_2–EtOAc–MeOH gradient elution. The fraction (1.4 g) eluted with 9 : 1 CH_2Cl_2–EtOAc was separated by reversed-phase silica gel column chromatography (CC) eluting with a MeOH–H_2O gradient. The fraction (115 mg) eluted with 80% MeOH–H_2O was further separated by Sephadex LH-20 CC eluting with MeOH, and the resulting subfractions were combined and purified by semi-preparative RP HPLC (Agilent Zorbax SB-C18 column; 5 μm; 9.4 × 250 mm; 85% CH_3CN in H_2O for 20 min; 3 mL min^{-1}) to afford 1 (9.5 mg, t_R 17.5 min). The fraction (1.8 g) eluted with 4 : 1 CH_2Cl_2–EtOAc was separated by reversed-phase silica gel CC eluting with a MeOH–H_2O gradient. The fraction (100 mg) eluted with 80% MeOH–H_2O was further separated by Sephadex LH-20 CC eluting with MeOH, and the resulting subfractions were combined and purified by semipreparative RP HPLC (Agilent Zorbax SB-C18 column; 5 μm; 9.4 × 250 mm; 75% CH_3CN in H_2O for 35 min; 3 mL min^{-1}) to afford 5 (5.5 mg, t_R 29.5 min). The fraction (2.0 g) eluted with 3 : 2 CH_2Cl_2–EtOAc was separated by reversed-phase silica gel CC eluting with a MeOH–H_2O gradient. The fraction (105 mg) eluted with 80% MeOH–H_2O was further separated by Sephadex LH-20 CC eluting with MeOH, and the resulting subfractions were combined and purified by semipreparative RP HPLC (Agilent Zorbax SB-C18 column; 5 μm; 9.4 × 250 mm; 82% CH_3OH in H_2O for 30 min; 3 mL min^{-1}) to afford 2 (10.2 mg, t_R 27.0 min). The fraction (185 mg) eluted with 90% MeOH–H_2O was further separated by Sephadex LH-20 CC eluting with MeOH, and the resulting subfractions were combined and purified by semi-preparative RP HPLC (Agilent Zorbax SB-C18 column; 5 μm; 9.4 × 250 mm; 80% CH_3CN in H_2O for 35 min; 3 mL min^{-1}) to afford 4 (4.0 mg, t_R 22.5 min), 3 (4.5 mg, t_R 25.0 min), and 6 (1.8 mg, t_R 29.5 min).

Shearinine U (2). Pale yellow amorphous powder; $[\alpha]_D^{25}$ − 116.9 (c 0.1, MeOH); UV (MeOH) λ_{max} (log ε) 225 (4.06), 282 (4.02) nm; CD (c 3.3×10^{-4} M, MeOH) λ_{max} ($\Delta\varepsilon$) 218 (−4.18), 244 (+5.80), 290 (−15.50) 360 (−2.76) nm; IR (neat) ν_{max} 3295 (br), 2973, 2930, 1657, 1593, 1456, 1380, 1255, 1131, 1023 cm^{-1}; ^{1}H and ^{13}C NMR data see Tables 1 and 2; HMBC data (DMSO-d_6, 600 MHz) H_2-6 → C-4, 7; H-9 → C-7, 10, 34, 35, 36; H-11 → C-7, 9, 12, 13; H-14 → C-4, 16; H-15a → C-13, 14; H-15b → C-13, 14; H-17a → C-2, 3, 16, 18; H-17b → C-2, 16, 18; H-20 → C-18, 19, 22, 29, 31; H-22 → C-21, 23, 28, 29; H-27 → C-23, 26, 29; H-30 → C-19, 21, 28; H_3-32 → C-2, 3, 4, 16; H_3-33 → C-3, 4, 5, 13; H_3-35 → C-9, 34, 36; H_3-36 → C-9, 34, 35; H_3-37 → C-23, 24, 38; H_3-38 → C-23, 24, 37; H_3-39 → C-26, 27, 40; H_3-40 → C-26, 27, 39; NH-1 → C-2, 18, 19, 31; OH-7 → C-7, 12; OH-34 → C-9, 34, 35, 36; NOESY correlations (DMSO-d_6, 600 MHz) H-9 ↔ OH-7; H-16 ↔ H-17a, H_3-33; H-17b ↔ H_3-32; HRESIMS m/z 604.3058 [M + Na]$^+$ (calcd for $C_{37}H_{43}NO_5Na$, 604.3033).

Shearinine V (3). Pale yellow amorphous powder; $[\alpha]_D^{25}$ − 85.7 (c 0.1, MeOH); UV (MeOH) λ_{max} (log ε) 248 (3.97) nm; CD (c 2.0×10^{-4} M, MeOH) λ_{max} ($\Delta\varepsilon$) 216 (−2.35), 243 (+3.61), 290 (−10.71) 358 (−1.99) nm; IR (neat) ν_{max} 3460 (br), 2972, 2933, 1671, 1456, 1375, 1255, 1137, 1033 cm^{-1}; ^{1}H and ^{13}C NMR data see Tables 1 and 2; HMBC data (DMSO-d_6, 600 MHz) H-9 → C-7, 10, 34, 35, 36; H-11 → C-7, 9, 13; H-17a → C-2, 3, 18; H-17b → C-2, 3, 18; H-20 → C-18, 22, 29, 31; H-22 → C-21, 28, 29; H-27 → C-23, 26, 29; H-30 → C-19, 21, 28; H_3-32 → C-2, 3, 4; H_3-33 → C-3, 4, 5, 13; H_3-35 → C-9, 34, 36; H_3-36 → C-9, 34, 35; H_3-37 → C-23, 24, 38; H_3-38 → C-23, 24, 37; H_3-39 → C-26, 27, 40; H_3-40 → C-26, 27, 39; NH-1 → C-2, 18, 19, 31; OCH_3-7 → C-7; OH-34 → C-34, 35, 36; NOESY correlations (DMSO-d_6, 600 MHz) H-9 ↔ OCH_3-7; H-16 ↔ H-17a, H_3-33; H-17b ↔ H_3-32; HRESIMS m/z 594.3225 [M–H]$^-$ (calcd for $C_{38}H_{44}NO_5$, 594.3225).

Shearinine W (4). Yellow amorphous powder; $[\alpha]_D^{25}$ + 14.3 (c 0.1, MeOH); UV (MeOH) λ_{max} (log ε) 207 (4.11), 234 (4.24) nm; CD (c 5.0×10^{-4} M, MeOH) λ_{max} ($\Delta\varepsilon$) 212 (−7.45), 240 (+7.02), 283 (−3.61) nm; IR (neat) ν_{max} 3359 (br), 2930, 1669, 1456, 1374, 1255, 1133, 1020 cm^{-1}; ^{1}H and ^{13}C NMR data see Tables 1 and 2; HMBC data (DMSO-d_6, 600 MHz) H-9 → C-7, 10, 34, 35, 36; H-11 → C-7, 9, 13; H-17a → C-2, 3, 18; H-17b → C-2, 3, 18; H-20 → C-18, 22, 29, 31; H-22 → C-21, 23, 24, 28, 29; H-27 → C-23, 26, 29, 39, 40; H-30 → C-19, 21, 28; H_3-32 → C-2, 3, 4, 16; H_3-33 → C-3, 4, 5, 13; H_3-35 → C-9, 34, 36; H_3-36 → C-9, 34, 35; H_3-37 → C-23, 24, 38; H_3-38 → C-23, 24, 37; H_3-39 → C-26, 27, 40; H_3-40 → C-26, 27, 39; NH-1 → C-2, 18, 19, 31; OCH_3-7 → C-7; OH-13 → C-4, 12, 13, 14; OH-34 → C-34, 35, 36; NOESY correlations (DMSO-d_6, 600 MHz) H-9 ↔ 7-OH; H-16 ↔ H-17a, H_3-33; H-17b ↔ H_3-32; HRESIMS m/z 614.3478 [M + H]$^+$ (calcd for $C_{38}H_{48}NO_6$, 614.3476).

Shearinine X (5). Yellow amorphous powder; $[\alpha]_D^{25}$ − 20.0 (c 0.1, MeOH); UV (MeOH) λ_{max} (log ε) 225 (3.66), 283 (3.77) nm; CD (c 1.5×10^{-4} M, MeOH) λ_{max} ($\Delta\varepsilon$) 229 (+2.32), 251 (+2.89), 282 (−1.57), 324 (+4.15), 373 (−3.87) nm; IR (neat) ν_{max} 3390 (br), 2974, 2932, 1661, 1456, 1374, 1257, 1168, 1134 cm^{-1}; ^{1}H and ^{13}C NMR data see Tables 1 and 2; HMBC data (DMSO-d_6, 600 MHz) H-5a → C-4, 6, 7, 33; H-5b → C-4, 6, 7, 13, 33; H-9 → C-7, 10, 34, 35, 36; H-11 → C-7, 9, 13; H-14 → C-4, 16; H-15a → C-3, 13; H-15b → C-3, 13; H-17a → C-2, 3, 18; H-17b → C-2, 3, 18; H-20 → C-18, 19, 22, 29, 31; H-22 → C-21, 23, 28, 29; H-27 → C-23, 26, 29, 39, 40; H-30 → C-19, 21, 28; H_3-32 → C-2, 3, 4,

16; H_3-33 → C-3, 4, 5, 13; H_3-35 → C-9, 34, 36; H_3-36 → C-9, 34, 35; H_3-37 → C-23, 24, 38; H_3-38 → C-23, 24, 37; H_3-39 → C-26, 27, 40; H_3-40 → C-26, 27, 39; NH-1 → C-2, 18, 19, 31; OH-13 → C-4, 13, 14; OH-34 → C-9, 34, 35, 36; NOESY correlations (DMSO-d_6, 600 MHz) H-16 ↔ H-17a, H_3-33; H-17b ↔ H_3-32; H_3-32 ↔ OH-13 HRESIMS m/z 582.3224 $[M + H]^+$ (calcd for $C_{37}H_{44}NO_5$, 582.3214).

Shearinine Y (6). Yellow amorphous powder; $[\alpha]_D^{25}$ + 90.2 (*c* 0.1, MeOH); UV (MeOH) λ_{max} (log ε) 290 (4.10), 365 (3.23) nm; CD (*c* 5.0 × 10^{-4} M, MeOH) λ_{max} ($\Delta\varepsilon$) 209 (+3.47), 301 (−8.29), 363 (+3.45) nm; IR (neat) ν_{max} 3285, 2974, 2916, 1663, 1456, 1379, 1252, 1130, 1060 cm^{-1}; ^{1}H and ^{13}C NMR data see Tables 1 and 2; HMBC data (DMSO-d_6, 600 MHz) H-9 → C-7, 10; H-11 → C-7, 9, 13; H-17a → C-2, 3, 18; H-17b → C-2, 3, 18; H-20 → C-18, 22, 29, 31; H-22 → C-21, 23, 28, 29; H-27 → C-23, 26, 29; H-30 → C-19, 21, 28; H_3-32 → C-2, 3, 4, 16; H_3-33 → C-3, 4, 5, 13; H_3-35 → C-9, 34, 36; H_3-36 → C-9, 34, 35; H_3-37 → C-23, 24, 38; H_3-38 → C-23, 24, 37; H_3-39 → C-26, 27, 40; NH-1 → C-2, 18, 19, 31; NOESY correlations (DMSO-d_6, 600 MHz) H-16 ↔ H-17a, H_3-33; H-17b ↔ H_3-32; HRESIMS m/z 564.3106 $[M + H]^+$ (calcd for $C_{37}H_{42}NO_4$, 564.3108).

Computational details

Conformational analyses for **2** and **4–6** within an energy window of 3.0 kcal mol^{-1} were performed by using the OPLS3 molecular mechanics force field. The conformers were then further optimized with the software package Gaussian 09 at the B3LYP/6-311G(2d,2p) level. Then the 60 lowest electronic transitions for the obtained conformers were calculated using time-dependent density functional theory (TD-DFT) methods at the CAM-B3LYP/6-311G(2d,2p) level. ECD spectra of the conformers were simulated using a Gaussian function. The overall theoretical ECD spectra were obtained according to the Boltzmann weighting of each conformer.[30]

Cytotoxicity assays. MTT assays were performed as previously described.[26] Briefly, cells were seeded into 96-well plates at a density of 5 × 10³ cells per well for 24 h and were exposed to different concentrations of test compounds. After incubation for 72 h, cells were stained with 25 μL of MTT solution (5 mg mL^{-1}) for 25 min. Finally, the mixture of medium and MTT solution was removed, and 75 μL of DMSO was added to dissolve formazan crystals. Absorbance of each well was measured at 544 nm (test wavelength) and 690 nm (background) using the multi-mode microplate reader. Background was subtracted from the absorbance of each well. Three duplicate wells were used for each concentration, and all the tests were repeated three times.

Conclusions

In summary, five new indole diterpenoids, shearinines U–Y (**2–6**), and a structurally related known compound 22,23-dehydroshearinine A (**1**) were isolated from cultures of the entomogenous fungus *Penicillium* sp. Their structures were elucidated based on NMR spectroscopic data and electronic circular dichroism (ECD) calculations. Compounds **2–5** differ from the known precedent by lacking the 1,3-dioxolane ring.[26] In addition, compound **3** is a C-7 methoxy product of **2**, **4** is a C-13 hydroxy product and C-14 alkylation of **3**, while **5** is a C-6–C-7 alkenyl product of **4**. Compound **6** is a C-13–C-14 alkenyl product of **1**. Compounds **1–3** showed moderate cytotoxicity, with IC$_{50}$ values of 11.7–26.2 μM. The shearinines exhibit certain chemical structures or properties that are shared among *Penicillium* strains and others. These shared chemical characteristics could be an indication of a common origin or a close evolutionary relationship.[8,31] Biogenetically, **1–6** could be originated from the copalyl diphosphate (CPP) synthases *via* the precursor (*E*,*E*,*E*)-geranylgeranyl diphosphate (GGDP) and tryptophan,[10,32,33] and the hypothetical biosynthetic pathways leading to the generation of these metabolites are illustrated in Scheme S1.†

Data availability

The data supporting the findings of this study are available within the article and/or its ESI.†

Conflicts of interest

The authors declare no conflict interest.

Acknowledgements

Notes and references

1 M. A. Corsello, J. Kim and N. K. Garg, *Chem. Sci.*, 2017, **8**, 5836–5844.

2 J. Niu, J. Qi, P. Wang, C. Liu and J. Gao, *Nat. Prod. Bioprospect.*, 2023, **13**, 3.

3 X. Hu, L. Meng, X. Li, S. Yang, X. Li and B. Wang, *Mar. Drugs*, 2017, **15**, 137.

4 O. F. Smetanina, A. I. Kalinovsky, Y. V. Khudyakova, M. V. Pivkin, P. S. Dmitrenok, S. N. Fedorov, H. Ji, J. Kwak and T. A. Kuznetsova, *J. Nat. Prod.*, 2007, **70**, 2054.

5 T. Yamaguchi, K. Nozawa, T. Hosoe, S. Nakajima and K. Kawai, *Phytochemistry*, 1993, **32**, 1177–1181.

6 P. Zhang, X. Li, X. Li and B. Wang, *Phytochem. Lett.*, 2015, **12**, 182–185.

7 S. Uhlig, W. Egge-Jacobsen, T. Vrålstad and C. O. Miles, *Rapid Commun. Mass Spectrom.*, 2014, **28**, 1621–1634.

8 C. A. Young, B. A. Tapper, K. May, C. D. Moon, C. L. Schardl and B. Scott, *Appl. Environ. Microbiol.*, 2009, **75**, 2200–2211.

9 T. Kawahara, A. Nagai, M. Takagi and K. Shin-ya, *J. Antibiot.*, 2012, **65**, 535–538.

10 Y. Fan, Y. Wang, P. Liu, P. Fu, T. Zhu, W. Wang and W. Zhu, *J. Nat. Prod.*, 2013, **76**, 1328–1336.

11 G. N. Belofsky, J. B. Gloer, D. T. Wicklow and P. F. Dowd, *Tetrahedron*, 1995, **51**, 3959–3968.

12 N. P. Ariantari, E. Ancheeva, C. Wang, A. Mándi, T. Knedel, T. Kurtán, C. Chaidir, W. E. G. Müller, M. U. Kassack, C. Janiak, G. Daletos and P. Proksch, *J. Nat. Prod.*, 2019, **82**, 1412–1423.

13 L. Dai, L. Yang, F. Kong, Q. Ma, Q. Xie, H. Dai, Z. Yu and Y. Zhao, *Mar. Drugs*, 2021, **19**, 613.

14 S. Pang, Z. Guo, L. Wang, Q. Guo and F. Cao, *Nat. Prod. Res.*, 2022, **37**, 586–591.

15 B. Chaiyosang, K. Kanokmedhakul, N. Yodsing, S. Boonlue, J. Yang, Y. A. Wang, R. J. Andersen, J. Yahuafai and S. Kanokmedhakul, *Nat. Prod. Res.*, 2021, **36**, 1–9.

16 G. Zhou, C. Sun, X. Hou, Q. Che, G. Zhang, Q. Gu, C. Liu, T. Zhu and D. Li, *J. Org. Chem.*, 2021, **86**, 2431–2436.

17 Z. Liang, N. Shen, X. Zhou, Y. Zheng, M. Chen and C. Wang, *Chem. Nat. Compd.*, 2020, **56**, 379–382.

18 A. C. D. Carvalho, C. Y. O. Junior, L. D. C. Rodrigues, L. S. D. Medeiros and T. A. M. Veiga, *Leuk. Lymphoma*, 2021, **62**, 2079–2093.

19 R. Nicoletti, A. Andolfi, A. Becchimanzi and M. M. Salvatore, *Microorganisms*, 2023, **11**, 1302.

20 R. M. K. Toghueo and F. F. Boyom, *3 Biotech.*, 2020, **10**, 107.

21 S. Liu, M. Su, S. Song and J. H. Jung, *Mar. Drugs*, 2017, **15**, 329.

22 M. Koul and S. Singh, *Anti-Cancer Drugs*, 2017, **28**, 11–30.

23 E. Li, F. Zhang, S. Niu, X. Liu, G. Liu and Y. Che, *Org. Lett.*, 2012, **14**, 3320–3323.

24 Y. Feng, L. Wang, S. Niu, L. Li, Y. Si, X. Liu and Y. Che, *J. Nat. Prod.*, 2012, **75**, 1339–1345.

25 F. Ren, S. Chen, Y. Zhang, S. Zhu, J. Xiao, X. Liu, R. Su and Y. Che, *J. Nat. Prod.*, 2018, **81**, 1752–1759.

26 J. You, L. Du, J. B. King, B. E. Hall and R. H. Cichewicz, *ACS Chem. Biol.*, 2013, **8**, 840–848.

27 S. Zhu, F. Ren, Z. Guo, J. Liu, X. Liu, G. Liu and Y. Che, *J. Nat. Prod.*, 2019, **82**, 462–468.

28 A. Saidykhan, W. H. C. Martin, R. T. Gallagher, J. Kendrick and R. D. Bowen, *J. Mol. Struct.*, 2023, **1294**, 136311.

29 N. Zhang, Y. Chen, R. Jiang, E. Li, X. Chen, Z. Xi, Y. Guo, X. Liu, Y. Zhou, Y. Che and X. Jiang, *Autophagy*, 2011, **7**, 598–612.

30 M. J. Frisch, G. W. Trucks, H. B. Schlegel, G. E. Scuseria, M. A. Robb, J. R. Cheeseman, G. Scalmani, V. Barone, B. Mennucci, G. A. Petersson, H. Nakatsuji, M. Caricato, X. Li, H. P. Hratchian, A. F. Izmaylov, J. Bloino, G. Zheng, J. L. Sonnenberg, M. Hada, M. Ehara, K. Toyota, R. Fukuda, J. Hasegawa, M. Ishida, T. Nakajima, Y. Honda, O. Kitao, H. Nakai, T. Vreven, J. A. Montgomery Jr, J. E. Peralta, F. Ogliaro, M. Bearpark, J. J. Heyd, E. Brothers, K. N. Kudin, V. N. Staroverov, R. Kobayashi, J. Normand, K. Raghavachari, A. Rendell, J. C. Burant, S. S. Iyengar, J. Tomasi, M. Cossi, N. Rega, J. M. Millam, M. Klene, J. E. Knox, J. B. Cross, V. Bakken, C. Adamo, J. Jaramillo, R. Gomperts, R. E. Stratmann, O. Yazyev, A. J. Austin, R. Cammi, C. Pomelli, J. W. Ochterski, R. L. Martin, K. Morokuma, V. G. Zakrzewski, G. A. Voth, P. Salvador, J. J. Dannenberg, S. Dapprich, A. D. Daniels, O. Farkas, J. B. Foresman, J. V. Ortiz, J. Cioslowski and D. J. Fox, *Gaussian 09, Rev D.01*, Gaussian, Inc., Wallingford, CT, 2009.

31 X. Wang, Z. Chen, J. Zhang, L. Hai, R. Ma, X. Liu, M. Li, D. Ge, J. Bao and H. Zhang, *Mar. Drugs*, 2023, **21**, 593.

32 C. Liu, A. Minami, T. Dairi, K. Gomi, B. Scott and H. Oikawa, *Org. Lett.*, 2016, **18**, 5026–5029.

33 R. M. McLellan, R. C. Cameron, M. J. Nicholson and E. J. Parker, *Org. Lett.*, 2022, **24**, 2332–2337.